Multi-agent Radio SLAM: A Point Cloud-based Approach

Seyeon Lee, Kyeong-Ju Cha, Hyunwoo Park, and Sunwoo Kim Department of Electronic Engineering, Hanyang University, Seoul, South Korea E-mail: {leah0900, lovelyckj, stark95, remero}@hanyang.ac.kr

Abstract—This paper proposes a multi-agent radio simultaneous localization and mapping (SLAM) employing a point cloud-based approach to enhance the accuracy, speed, and stability of the mapping. Traditional radio SLAM relies on measurements from a single sensing source, resulting in low reliability and limited sensing coverage. To overcome these challenge, the proposed algorithm fuses local maps of individual user equipments (UEs) through a point cloud-based approach. In a scenario with two moving UEs, the simulation results demonstrate that the angular error converges to a smaller value at a faster rate, and the Chamfer distance reaches zero nearly twice as fast compared to the single-agent cases.

Index Terms—Radio simultaneous localization and mapping, multi-agent, point cloud

I. INTRODUCTION

Radio Simultaneous localization and mapping (SLAM) estimates the current position of user equipment (UE) while constructing a map of the surrounding environment employing radio signals [1], [2]. Radio SLAM operating with a single UE relies on measurements from only one sensing source, resulting in low reliability and limited coverage [3], [4]. To overcome these limitations, this paper proposes a multi-agent radio SLAM employing a point cloud-based approach, where multiple UEs fuse their locally estimated maps to improve both accuracy and speed. The point cloud-based approach accumulates reflection points (RPs) and processes them collectively to achieve stable mapping, providing realistic and visually interpretable locations.

II. System Model

This paper considers a scenario with a single base station (BS) and N UEs for localization and mapping, as illustrated in Fig. \blacksquare The fixed position of the BS is denoted by $\mathbf{p}_{\mathrm{BS}} = [x_{\mathrm{BS}}, y_{\mathrm{BS}}]^{\top}$ and each UE is assumed to be mounted on a vehicle. The state of the n-th vehicle at time t is defined as $\mathbf{s}_{n,t} = [\mathbf{p}_{\mathrm{UE},n,t}^{\top}, \alpha_{n,t}, \rho_{n,t}, \zeta_{n,t}, \zeta_{n,t}]^{\top}$, where $\mathbf{p}_{\mathrm{UE},n,t} = [x_{\mathrm{UE},n,t}, y_{\mathrm{UE},n,t}]^{\top}$ is the 2D position of the n-th UE, $\alpha_{n,t}$ is the heading, $\rho_{n,t}$ is the translation speed, $\zeta_{n,t}$ is the turn-rate, and $\xi_{n,t}$ is the clock bias. The dynamic model of the n-th vehicle is given by

$$\mathbf{s}_{n,t} = \mathbf{v}(\mathbf{s}_{n,t-1}) + \mathbf{e}_{n,t},\tag{1}$$

This work was supported by Institute of Information & communications Technology Planning & Evaluation (IITP) grant funded by the Korea government (MSIT) (No. RS-2024-00428780, 6G-Cloud Research and Education Onen Hub)

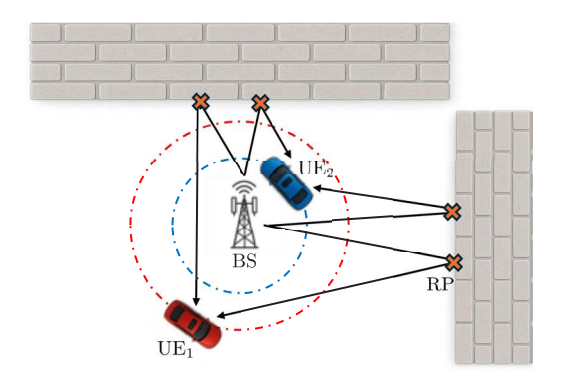


Fig. 1. An Example of multi-agent radio SLAM.

where $\mathbf{v}(\cdot)$ is a known transition function $\boxed{\mathbf{5}}$ and $\mathbf{e}_{n,t}$ denotes the process noise with known covariance \mathbf{E} .

Each UE receives a line-of-sight (LOS) signal and non-line-of-sight (NLOS) signals reflected from K walls. The corresponding measurements are modeled as

$$[\hat{d}_{k,n,t}, \hat{\theta}_{k,n,t}]^{\top} = [d_{k,n,t}, \theta_{k,n,t}]^{\top} + \mathbf{r}$$
 (2)

where $\mathbf{r} \sim \mathcal{N}(0,\mathbf{R})$ denotes the measurement noise with known covariance $\mathbf{R}.$ $d_{k,n,t}$ and $\theta_{k,n,t}$ are the true propagation distance and true angle-of-arrival (AOA), respectively. The parameters of the LOS and the k-th NLOS paths are given by

$$\begin{aligned} d_{k,n,t} & & (3) \\ &= \begin{cases} \|\mathbf{p}_{\text{BS}} - \mathbf{p}_{\text{UE},n,t}\|, & k = 0 \\ \|\mathbf{p}_{\text{BS}} - \mathbf{p}_{\text{RP},k,n,t}\| + \|\mathbf{p}_{\text{RP},k,n,t} - \mathbf{p}_{\text{UE},n,t}\|, & \text{otherwise} \end{cases} \end{aligned}$$

$$\theta_{k,n,t} = \begin{cases} \arctan \frac{\mathbf{p}_{BS} - \mathbf{p}_{UE,n,t}}{\|\mathbf{p}_{BS} - \mathbf{p}_{UE,n,t}\|}, & k = 0\\ \arctan \frac{\mathbf{p}_{RP,k,n,t} - \mathbf{p}_{UE,n,t}}{\|\mathbf{p}_{RP,k,n,t} - \mathbf{p}_{UE,n,t}\|}, & \text{otherwise} \end{cases}$$
(4)

where $\mathbf{p}_{\text{RP},k,n,t} = [x_{\text{RP},k,n,t},y_{\text{RP},k,n,t}]^\top$ is the position of RP.

III. MULTI-AGENT RADIO SLAM

A. Localization

For UE positioning, the Jacobian matrix, derived from the measurements obtained through the case with the smallest \hat{d}

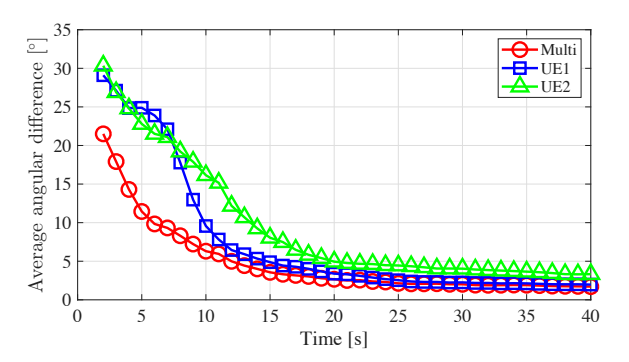


Fig. 2. Comparison of the average angular difference between the proposed multi-agent and single-agent SLAM.

value, is given by

$$\mathbf{J} = \begin{bmatrix} \cos(\hat{\theta}_{0,n,t}) & -\hat{d}_{0,n,t} \cdot \sin(\hat{\theta}_{0,n,t}) \\ \sin(\hat{\theta}_{0,n,t}) & \hat{d}_{0,n,t} \cdot \cos(\hat{\theta}_{0,n,t}) \end{bmatrix}, \tag{5}$$

and is used to compute the measurement coordinate covariance $\mathbf{O} = \mathbf{J}\mathbf{R}\mathbf{J}'$. The final estimated position of the UE is obtained as

$$\hat{\mathbf{p}}_{\mathrm{UE},n,t} = \mathbf{M}(\mathbf{G}^{-1} \cdot \mathbf{p}_{\mathrm{UE},n,t} + \mathbf{O}^{-1} \cdot \mathbf{p}_m), \tag{6}$$

where M denotes the fused covariance, G is the covariance of $\mathbf{p}_{\mathrm{UE},n,t}$, and \mathbf{p}_m is the position of the UE estimated from LOS path.

B. Mapping

Mapping is performed in all cases except for the one with the smallest \hat{d} value. Each path is assumed to involve a single bounce, where the signal propagates from the BS to a RP and then to the UE. The estimated position of the RP can be determined by

$$\begin{cases} \|\hat{\mathbf{p}}_{RP,k,n,t} - \mathbf{p}_{BS}\| + \|\hat{\mathbf{p}}_{RP,k,n,t} - \hat{\mathbf{p}}_{UE,n,t}\| = \hat{d}, \\ (\hat{\mathbf{p}}_{RP,k,n,t} - \hat{\mathbf{p}}_{UE,n,t})^{\mathsf{T}} \mathbf{u}_{k,n,t} = \|\hat{\mathbf{p}}_{RP,k,n,t} - \hat{\mathbf{p}}_{UE,n,t}\|, \end{cases}$$
(7)

where $\mathbf{u}_{k,n,t} = [\cos(\hat{\theta}_{k,n,t}), \sin(\hat{\theta}_{k,n,t})]^{\top}$ is the unit direction vector. The RP lies on an ellipse with the BS and the UE as its foci, and also on a straight line originating from the UE in the direction of the $\mathbf{u}_{k,n,t}$. The RP's position is determined by the intersection of the line and the ellipse.

C. Post-processing

K-means clustering is applied to partition the set of all mapped RPs into K non-overlapping clusters, each associated with a wall. The objective of clustering is given by $\operatorname{argmin}_k(\sum_{(k,n,t)}\|\hat{\mathbf{p}}_{\mathrm{RP},k,n,t}-\hat{\boldsymbol{\mu}}_k\|^2)$, where $\hat{\boldsymbol{\mu}}_k$ denotes centroid of the set of points in the k-th cluster. Principal component analysis (PCA) is then used for each cluster to determine the line that best fits its points. Each wall is estimated as the line passing through $\hat{\boldsymbol{\mu}}_k$ in the direction of the principal component vector $\hat{\boldsymbol{v}}_k$ as follows:

$$\hat{\mathbf{w}}_k = \hat{\gamma}_k \hat{\boldsymbol{v}}_k + \hat{\boldsymbol{\mu}}_k,\tag{8}$$

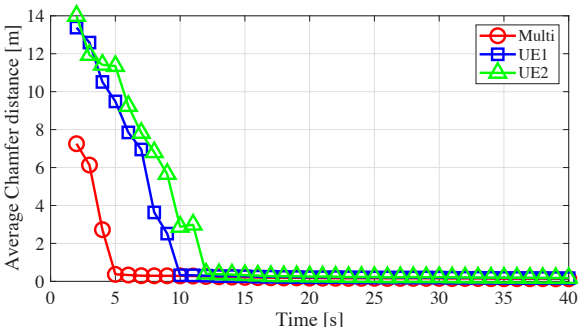


Fig. 3. Comparison of the average Chamfer distance between the proposed multi-agent and single-agent SLAM.

where the scalar $\hat{\gamma}_k$ is determined from the boundary points.

IV. SIMULATION RESULTS

An $120\,\mathrm{m}\times60\,\mathrm{m}$ indoor environment is considered with a fixed BS and two vehicles moving along different trajectories around it. The BS is located at $[0\,\mathrm{m},0\,\mathrm{m}]^{\top}$ and the each vehicle is initially set to $\mathbf{s}_{1,t}=[15.9\,\mathrm{m},\,0\,\mathrm{m},\,\pi/2\,\mathrm{rad},\,5\,\mathrm{m/s},\,\pi/10\,\mathrm{rad/s}]^{\top},\,\mathbf{s}_{2,t}=[7.9\,\mathrm{m},\,0\,\mathrm{m},\,\pi/2\,\mathrm{rad},\,2.5\,\mathrm{m/s},\,\pi/10\,\mathrm{rad/s}]^{\top}.$ The noise covariance matrix of the process E, the measurement covariance matrix R, and the position covariance matrix G are set to $\mathrm{diag}(0.04\,\mathrm{m}^2,0.04\,\mathrm{m}^2,10^{-6}\mathrm{rad}^2,0,0,0.04\,\mathrm{m}^2),\,\mathrm{diag}(9\,\mathrm{m}^2,10^{-2}rad^2),\,\,\mathrm{diag}(1\,\mathrm{m}^2,10^{-4}rad^2),\,\,\mathrm{respectively}.$ The total time is set to T=40, and the simulation is repeated 100 times to ensure statistical reliability.

To compare the similarity of the estimated wall and the ground truth (GT) wall, mapping performance is evaluated using the angular difference and the one-way Chamfer distance. The angular difference between the direction vector of the two walls is defined as $\frac{180}{\pi}\arccos(\boldsymbol{v}_k\cdot\hat{\boldsymbol{v}}_k)$, where \boldsymbol{v}_k denotes the direction vector of the k-th wall. For the Chamfer distance computation, the estimated wall and the corresponding GT segment obtained by projection are each sampled in 200 points, forming the points sets $L_{\rm est}$ and $Q_{\rm GT}$, respectively. The one-way Chamfer distance is defined as $\sum_{l\in L_{\rm est}} \min_{q\in Q_{\rm GT}} \|l-q\|$.

The mapping performance evaluation results are shown in Fig. 2 and Fig. 3 In Fig. 2 the proposed algorithm converges to a smaller value at a faster rate compared to the single-agent cases, indicating that it estimates a wall parallel to the GT. In Fig. 3 while the single-agent cases require more than 10s to reach zero, the proposed algorithm achieves convergence at approximately twice the speed, accurately estimating the wall at the same position as the GT. Consequently, based on both evaluation metrics, the multi-agent SLAM algorithm demonstrates faster, more accurate, and stable mapping results.

V. CONCLUSION

This paper proposes a multi-agent radio SLAM that employs a point cloud-based approach. By integrating local maps

from multiple UEs, the proposed algorithm achieves rapid mapping through accumulation of RPs, furthermore, refines the results with K-means and PCA for stable and accurate wall estimation. Compared to single-agent cases evaluated with angular difference and one-way Chamfer distance, the proposed algorithm converges to nearly zero error values significantly faster. The simulation results demonstrate the speed, accuracy, and stability of the proposed algorithm in mapping the surrounding environment.

REFERENCES

- [1] H. Que, J. Yang, T. Du, S. Xia, C.-K. Wen, and S. Jin, "Cooperative mapping, localization, and beam management via multi-modal slam in isac systems," *IEEE Trans. Commun.*, 2025.
- [2] L. Wielandner, E. Leitinger, F. Meyer, and K. Witrisal, "Message passing-based 9-d cooperative localization and navigation with embedded particle flow," *IEEE Trans. Signal Inf. Process. Netw.*, vol. 9, pp. 95–109, 2023.
- [3] E. Leitinger, F. Meyer, F. Hlawatsch, K. Witrisal, F. Tufvesson, and M. Z. Win, "A belief propagation algorithm for multipath-based slam," *IEEE Trans. Wireless Commun.*, vol. 18, no. 12, pp. 5613–5629, 2019.
- Trans. Wireless Commun., vol. 18, no. 12, pp. 5613–5629, 2019.
 [4] J. Yang, C.-K. Wen, J. Xu, H. Que, H. Wei, and S. Jin, "Angle-based slam on 5g mmwave systems: Design, implementation, and measurement," IEEE Internet Things J., vol. 10, no. 20, pp. 17755–17771, 2023.
- IEEE Internet Things J., vol. 10, no. 20, pp. 17755–17771, 2023.
 [5] S. T. et al., "Probabilistic robotics," Commun. of the ACM, vol. 45, no. 3, pp. 52–57, 2002.